Current State of NASA Continuously Rotating Detonation Cycle Engine Development

Thomas Teasley[1], Tessa Fedotowsky[2], Paul Gradl[3]
NASA Marshall Space Flight Center, Huntsville, AL, 35808, United States

Benjamin Austin[4] and Stephen Heister[5]
IN Space, LLC, West Lafayette, IN, 47906, United States
Purdue University, West Lafayette, IN, 47906, United States

NASA is currently investigating continuous detonation cycle engines for the application of lander and interplanetary space exploration missions. The performance benefits of a detonation cycle engine may allow for a broader design trade space and more compact geometry required for future missions to the Moon and onwards towards Mars. However, the technology readiness level (TRL) within the US was found to be low with several major risk factors that require understanding prior to full engine system development. One area of uncertainty is the extreme heat loads expected during thermal steady state conditions. To achieve this, an announcement for collaborative opportunity (ACO) partnership between IN Space LLC and NASA Marshall Space Flight Center (MSFC) was established to explore integration of additive manufacturing (AM) processes and the high conductance copper-based alloys, GRCop-42 and GRCop-84. This work outlines the hot fire testing of a 7K lbf thrust class fully AM GRCop-alloy rotating detonation rocket engine (RDRE). Two annular thrust chamber configurations emulating a lander engine system were tested with LOx/GH2 and LOx/LCH4. In both configurations, select hardware was actively cooled using de-ionized water and regeneratively cooled using LCH4. All primary hardware survived long duration tests to thermal steady state up to 133 seconds in a single burn. In total, 18 starts and 802 seconds of duration were achieved with and without visual confirmation of waves present. The proportion of burned propellant, or level of complete combustion, was found to be high compared to the theoretically achievable mean chamber pressure in all cases.

I. Nomenclature

AM	=	additive manufacturing
CAD	=	computer aided design
CP	=	constant pressure
CTAP	=	capillary tube attenuated pressure
CASI	=	compact augmented spark igniter
*C**	=	characteristic exhaust velocity
DDT	=	deflagration to detonation
DI	=	de-ionized
EHV	=	electrohydraulic valve
GH2	=	gaseous hydrogen

[1] Combustion Devices Engineer, Engine Component Development and Technology Branch
[2] Propulsion Systems Structures and Design Engineer, Detailed Design Strength and Life Assessment Branch
[3] Principle Engineer, Associate Fellow AIAA, Engine Component Development and Technology Branch
[4] Senior Propulsion Systems Engineer, IN Space, LLC
[5] Senior Propulsion Systems Engineer, IN Space, LLC and Raisbeck Professor, Purdue University

Isp = specific impulse
L-PBF = laser powder bed fusion
LOx = liquid oxygen
LCH4 = liquid methane
*L** = chamber characteristic length (volume / throat area)
L' = distance from injector face to throat proper.
MSFC = Marshall Space Flight Center
MR = mixture ratio
NASA = National Aeronautics and Space Administration
PGC = pressure gain combustion
RDRE = rotating detonation rocket engine
RDE = rotating detonation engine
SOA = state of the art
TCA = thrust chamber assembly
TRL = technology readiness level

II. Introduction

Propulsion systems are continuously changing to provide higher-efficiency and improved performance for future missions such as lunar transit and a sustainable Lunar to Martian architecture. As current systems have been optimized for performance, these future missions may require unique propulsion concepts with new manufacturing processes and materials to meet the extreme environments. This work outlines efforts made at NASA Marshall Space Flight Center to experimentally quantify performances such as heat loads, duty cycle, combustion efficiency, detonation characteristics, and global engine thrust for Rotating Detonation Rocket Engine (RDRE) thrust chambers and injectors. The work presented in this paper was conducted as part of a NASA announcement for collaborative opportunity (ACO) award in partnership with IN Space, LLC and Purdue University. This project sought to rapidly advance RDRE technology within the US via integration of additive manufacturing (AM) processes and high performance (high conductivity and high strength) copper-based alloys, GRCop-42 and GRCop-84. The primary AM process used for manufacturing of hardware was the laser powder bed fusion process (L-PBF). The project leveraged the previously established NASA material and supply chain to build major components. This effort aimed to develop the engine technology towards a more flight-like configuration and rapidly advance the technology readiness level (TRL). At the start of this investigation, the TRL was approximately 3 with advancement towards 5 by its completion. The primary goal was to demonstrate continuous detonation modes, with cryogenic liquid propellants, and at long durations greater than 100 seconds. Liquid oxygen (LOx) in combination with liquid methane (LCH4) or gaseous hydrogen (GH2) were both explored in a phase 1 and phase 2 back-to-back test series during the summer of 2022.

Major achievements for this effort are as follows:

1. Multiple hot fires were achieved in two chamber configurations > 100 seconds with detonation wave modes, the longest being 133 seconds. This achievement completed the primary goal of the project.
2. A single high thrust test at 622 psia, as measured at the injector face, with detonation modes achieved up to 4171 lbf with LOX/GCH4.
3. Three tests successfully demonstrated liquid/liquid direct injection (LOX/LCH4) with co-rotating wave modes.
4. A novel integrated multi-point ignition system was successfully demonstrated to work with both LOX/GCH4 and LOX/H2 injection.
5. Active throttling was successful with wave modes between each power level.
6. Direct measurement of heat flux profiles with deflagrative and detonative modes were measured.
7. In many cases, combustor C* was found to be high and used as a measure to gauge completion of combustion. This work demonstrated 90+ percentage of complete combustion in a chamber geometry with extremely low L* and L'.

Images of pivotal hot fire tests are shown in Fig 1.

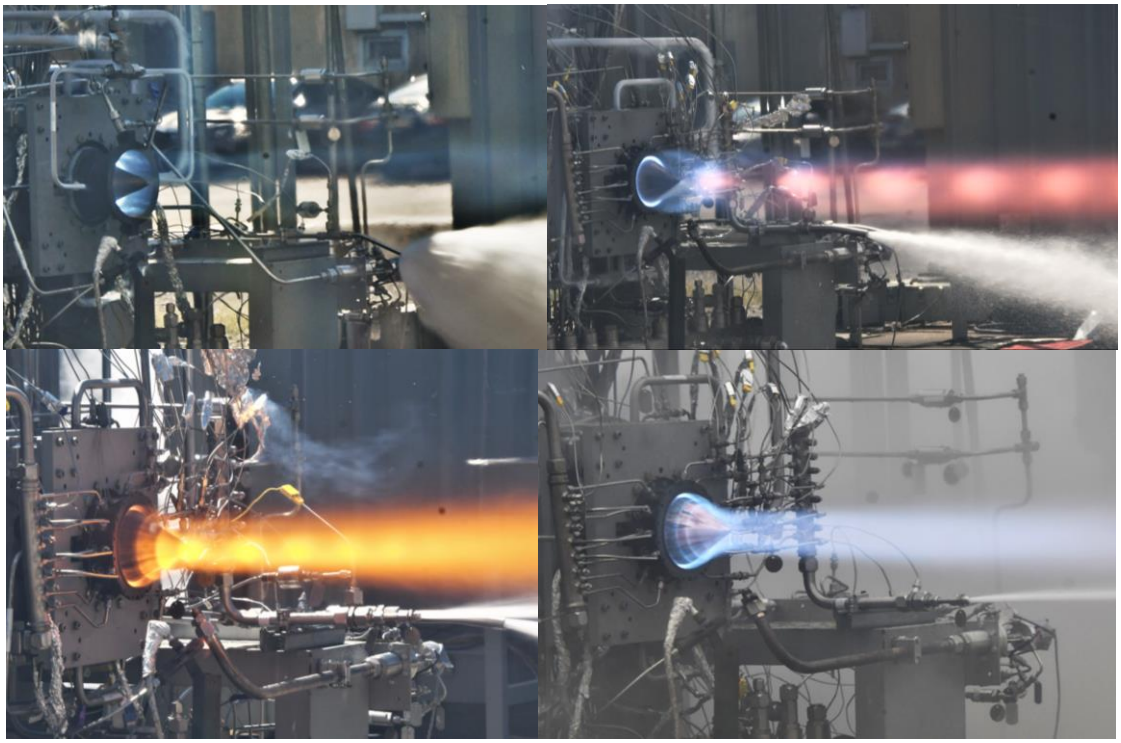

Fig 1. NASA RDRE pivotal hot fire tests; high pressure/ thrust test 019 LOX/CH4 at MR 3.74 (top left), high pressure test 028 direct injection LOX/LCH4 at MR 3.47 (top right), first successful ignition LOX/GH2 test 003 at MR 4.2 (bottom left), successful throttled test 024 with detonation modes at MR 2.2 (bottom right).

US research on RDRE's has focused on small scale, gas/gas injection, and for short duration (~1 s) firings typically due to limited funding or access to test facilities. To achieve this project's goals, two chamber variants were designed and constructed to obtain critical performance metrics of the detonative combustion cycle. The first chamber assembly (V1) was a typical straight annular configuration with radially running coolant channels for direct calorimetry measurement of heat flux profiles at axial stations along the hot wall. An image of this chamber CAD is given in Fig 4. These chamber solutions were specifically designed to be compact and push the bounds of what is possible in the AM L-PBF process. Many design features and challenges such as minimum wall thicknesses, complexity of powder removal, and instrumentation ports have not previously been attempted and were demonstrated to be possible under this work. The V1 was designed to operate with de-ionized water or regenerative cooling with cryogenic liquid methane (LCH4) fuel. The second chamber (V2) was a similar design but with more traditional [1] integrated axial running coolant channels and an integrated cowl extending to the exit plane of the plug nozzle. Typical rocket performance parameters were assumed to apply in the initial design phase. Images of hardware installation are shown in Fig 2.

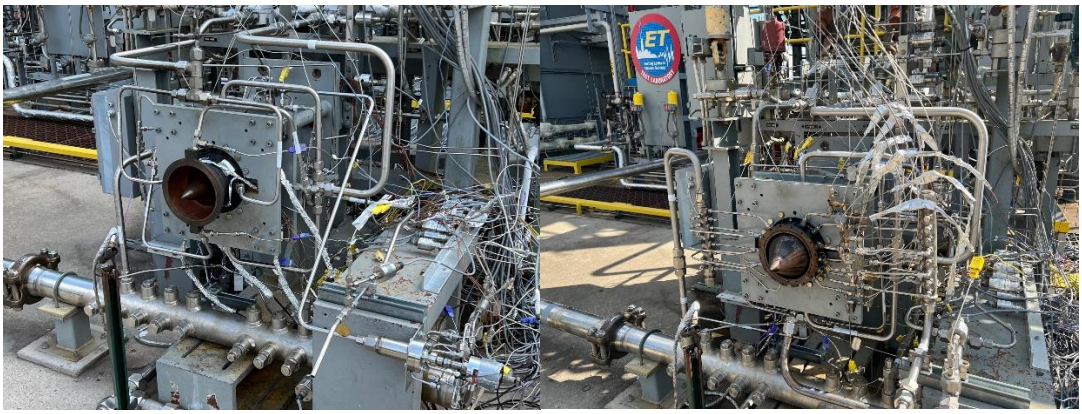

Fig 2. V2 RDRE (left) and V1 RDRE (right) as built-up on the TS115 stand.

Several major advantages of the RDRE over traditional liquid rocket geometries include its compact design trade space coupled, high rate of heat release, and rapid completion of combustion. This allows for chamber and nozzle geometries that are approximately 40-50% shorter than the current state of art (SOA). This was the case for a similar constant pressure (CP) thrust chamber when directly compared. Images of a comparable RDRE scheme and the NASA CP thrust chamber are shown in Fig 3 with identical supersonic area ratio nozzles.

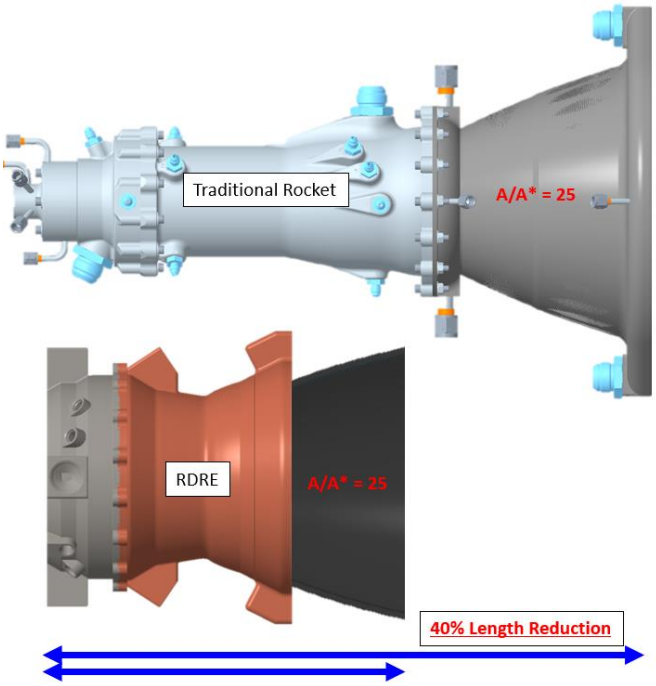

Fig 3. From left to right, NASA CP WHALE engine (top) and V2 RDRE (bottom).

The following sections give an overview of hardware geometry and design strategy.

A. Chamber and Injector Hardware

All chamber and injector hardware were produced using GRCop-42 (Cu-4Cr-2Nb) or GRCop-84 (Cu-8Cr-4Nb) where Chromium is 4% and 8% by mass, respectively and Niobium is 2% and 4% by mass, respectively. Each individual component was fabricated at a select additive powder bed fusion vendor within the US. In total, four separate vendors were utilized. This demonstrates the viability of the existing AM supply chain to produce large scale RDRE components. Other industry, government, or academic sources would be able to reliably use the supply chain for future component development. Table 1 summarizes the dimensions and relevant rocket parameters of the RDREs.

Table 1. Summary of Chamber Geometry

Overall length (in)	8.218
L', length from injector face to throat (in)	2.736
Volume from injector face to throat (in^3)	17.8
L* (in), chamber volume/throat area	2.9
Inner Body Diameter (in)	5.59
Annulus Gap Width G_c (in)	0.33
Expansion ratio, A_e/A_t	5.0

Fig 4 provides an exploded view of the V1 chamber assembly with specific components as-tested. Both assemblies utilize the identical injector design, interface, and thrust mount. The V1 is comprised of four components: an outer body, inner body, outer body nozzle, and inner body plug nozzle. All components with the exception of the

plug nozzle, are calorimetry based and can be used with methane or water as coolant. The V2 chamber is comprised of only two components: an inner body with coupled contoured plug nozzle and an outer body with a coupled bell type outer nozzle. The outer body utilized both DI water and LCH4 as coolant while the inner body was actively cooled using DI water only.

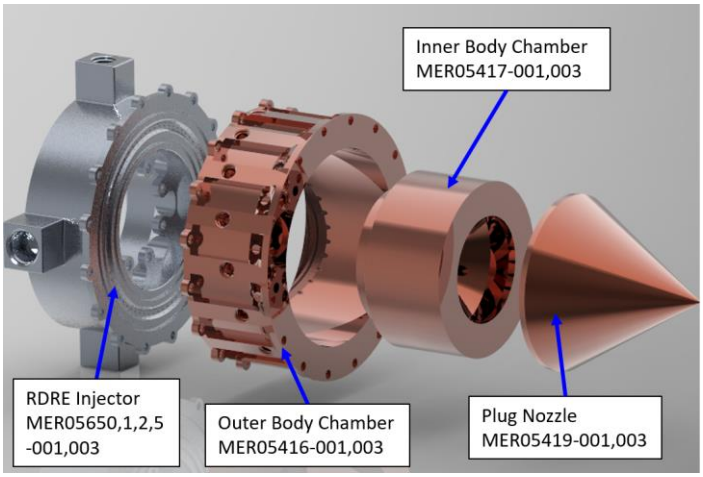

Fig 4. Variant 1 chamber assembly per MER05415-001. Labeled axial cut view (top left), canted cut view (top right), and exploded view (bottom).

Once all chamber assemblies were printed, heat treated, and post process machined they were proof tested and checked out for leaks. This was done to identify any unacceptable levels of porosity or potential failure points. Proofing was conducted up to 2500 psig for all chamber components. Finally, water flow testing was conducted on all test articles to obtain resistances, pressure drops, and identify if all coolant channels were free and clear of powder. Flow test images and buildup of chamber hardware are shown in Fig 5.

Fig 5. Channel flow testing (left) and buildup of hardware assemblies (right).

Once all proofing and flow testing was completed, the hot wall surfaces were polished via similar techniques reported in [1], [2], and the results are shown in Fig 6.

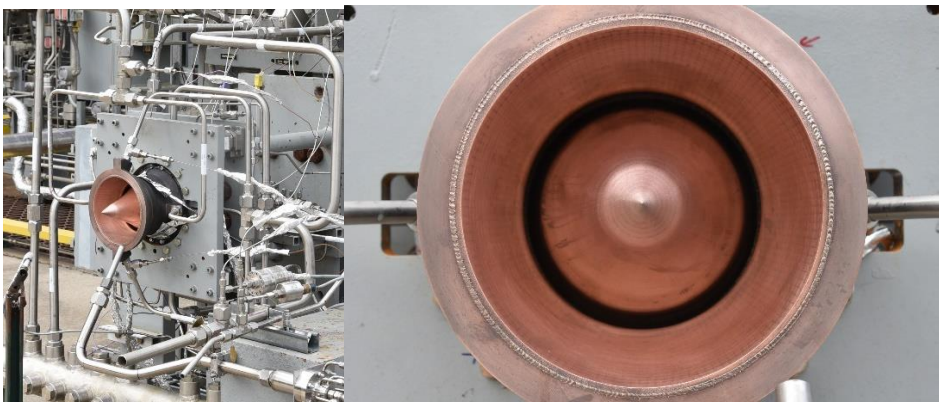

Fig 6. V2 hardware polished hot wall prior to hot fire test 012.

The thrust chamber assembly was then installed onto test stand 115 at Marshall's heritage east test area, as shown in Fig 6.

Similarly, injector hardware were also produced using the L-PBF process with GRCop-42, Alloy 718, and NASA Hydrogen Resistant Material 1 (HR-1). Only the GRCop-42 and Alloy 718 injectors were tested and are shown in Fig 7.

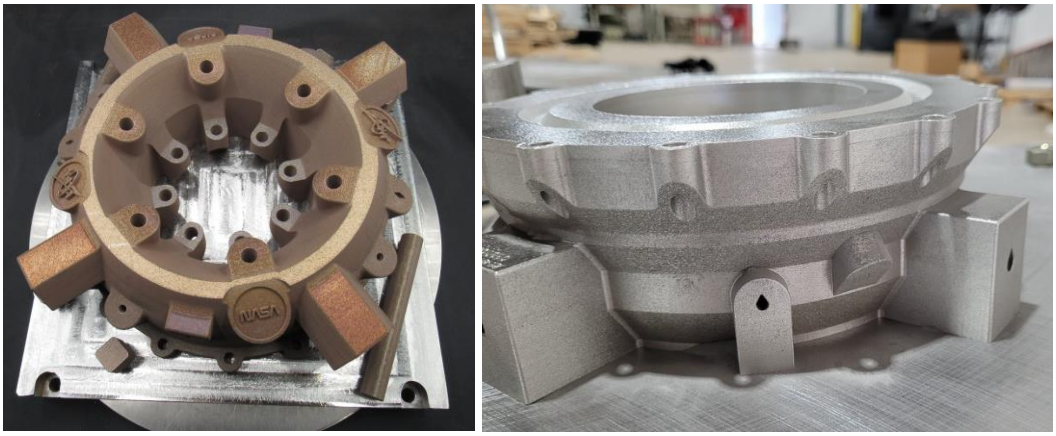

Fig 7. Injector body produced using L-PBF GRCop-42 (left) and Alloy 718 (right).

B. Ignition Methodology

NASAs compact augmented spark impinging (CASI) igniter previously utilized under nearly a dozen other NASA test projects since 2019 [3]–[7], was the primary means for ignition. The CASI igniter uses a GOX/GH2 deflagrative oxygen rich torch as opposed to pre-detonator typically used by other investigations [8]. Ignition was achieved for the V1 by backlighting externally and in the V2 by integrated igniter ports printed directly into the injector face. The backlight configuration was achieved by externally mounting a transfer tube that was routed to aim igniter combustion products into the annulus through the exit plane. In most cases, ignition was achieved. Alternatively, pyrophoric TEA/TEB was considered as a backup ignition methodology however was not required or explored. Images of the CASI used with the V1 and V2 configurations are shown in Fig 8 with annotations.

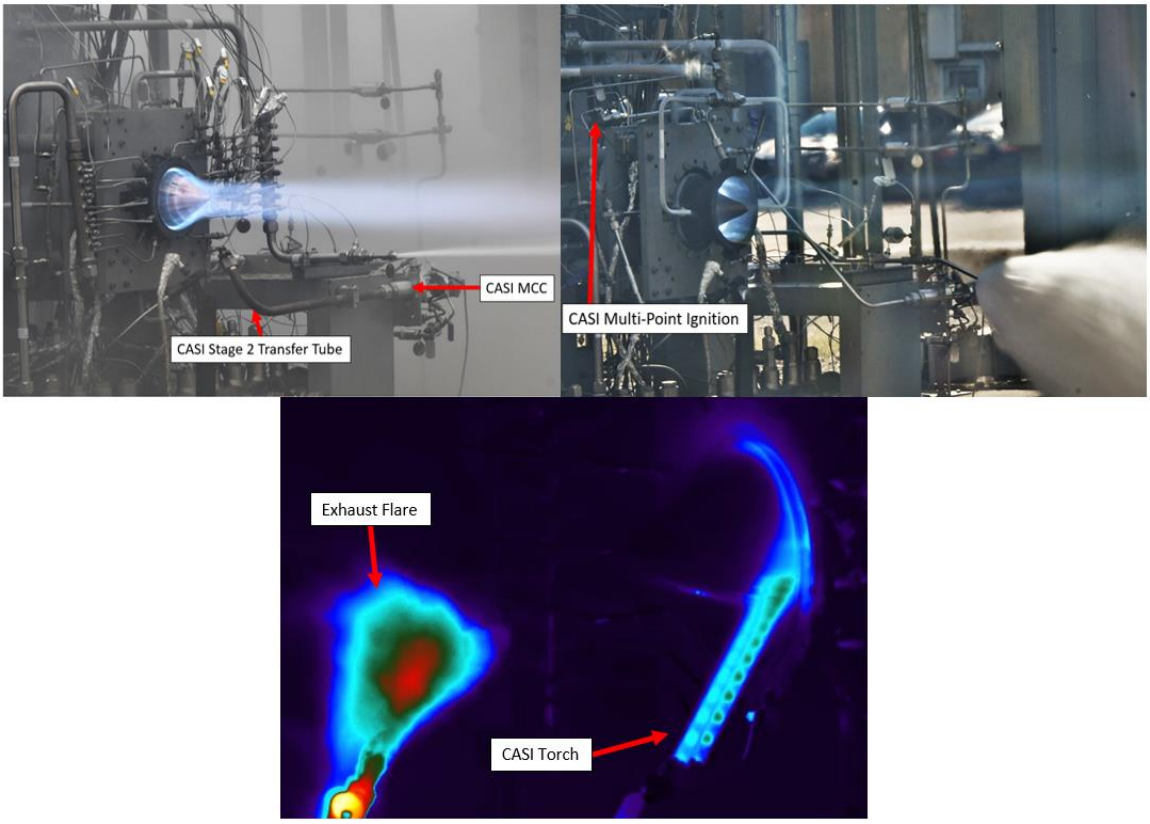

Fig 8. Test 024 V1 with CASI main combustion chamber (MCC) external ignition (top left), test 019 V2 with CASI multi-point integrated ignition (top right), and infrared image of external CASI ignition prior to main propellent injection (bottom).

The Fig 8 shows an infrared image of the torch igniter prior to injection of main propellants with hot combustion produces traveling around the annulus from the external source.

III. Experimental Design

This section discusses the experimental design and test capability of NASA's test stand 115 at Marshall Space Flight Center. The control sequence used under this investigation was capable of throttled cycle tests, where the main propellant electrohydraulic valves (EHV) could be opened and closed to specific percentage open values, thus metering the flow. For all ignition conditions, the valves were set to precalculated low values of 2-10% open depending on the upstream pressure to avoid "ram-starting" and achieving a "no ignition detect" condition. For all ignition cases, a stoichiometric mixture was targeted. Flow characterized venturis with throat taps are installed upstream of the main EHVs so that accurate calculation of mass flow rates could be obtained. This was the same way active throttling was achieved during mainstage. The main EHVs were toggled to a predefined open percentage and remained at that position for a set time. An example of throttling is shown in Fig 9.

Fig 9. Example of a typical throttled test where valves are toggled to yield a lower (left) and higher (right) power condition.

Several different hardware configurations were attempted with differing means of active and regenerative cooling of hardware, depending on the propellants of interest. These configurations are outlined and described in Table 2.

Table 2. Test configuration description

Configuration	Tests	Description
V1 Hydrogen	001-011	Water cooled hardware, direct GH2 injection, external ignition.
V2 Hydrogen	012	Water cooled hardware, direct GH2 injection, external ignition. Inner body failure due to clogged channels.
V2 Methane – Regen Outer Body	013-016	Methane regen outer body, water cooled inner body, internal ignition.
V2 Methane – Regen Outer Body	017-019	Methane regen outer body, water cooled inner body, internal ignition.
V1 Methane – Regen Inner Body	020-023	Water cooled outer body, methane regen inner body and bypass regen plug nozzle, external ignition.
V1 Methane – Mixer Regen Inner body	024-025	Water cooled outer body, methane regen inner body, bypass methane cooled plug nozzle dumped to burn stack, siphoned LCH4 mixed downstream within inner body exit manifold, external ignition.
V1 Methane – Direct Liquid Injection	026-028	Water cooled hardware, liquid methane direct injection.

Six different configurations were tested to identify critical performance parameters of the two RDRE chambers. When switching over to V1 methane, it was apparent that the water-cooled design was far too restrictive for methane regen and substantially limited the total mass flow rate of the fuel resulting in low mean chamber pressures. The final configuration was the direct liquid injection of methane and oxygen – the first experiment of this nature based on published available literature. This yielded clear wave activity with 2-3 waves and minimal visual deflagration between wave heads. Typical injection temperatures for LOx was approximately -270 F and for LCH4 approximately -220 F with a 10 degree variation maximum under stead state conditions.

C. Instrumentation and Diagnostics

A standard suite of pressure transducers capable of measurements ranging from 500-3000 psig maximum along with temperature probes were used on all propellant and coolant lines. All standard instrumentation measurements

were recorded at 100 samples per second with high speed recorded at the maximum rate of 100,000 samples per second.

One high-definition video camera, four standard definition viewing cameras, and several monochromatic infrared cameras were used at an angled vantage point downstream of the test position. In addition, low/high resolution still images were processed from a Nikon D850 DSLR cameras. A single GoPro camera was mounted to a vertical pole next to the test article for an arial vantage. Infrared thermography was also leveraged with the support of NASA MSFC ER43 with a dual forward looking infrared (FLIR) A655 body and FOL89 7-degree lens. A dual setup was used to capture both a high temperature regime and low temperature regime. Images of the IR videography setup are shown in Fig 10.

Fig 10. FLIR A655 body (top left) and dual imager setup with FOL89 7-degree lenses (top right), and diagram of FLIR placement (bottom).

Three high-speed cameras were utilized at unique vantage points. Two cameras were positioned to view the interior of the annulus to obtain wave imagery. One was positioned about 35 feet downstream and 6 feet off centerline, while the other was positioned about 20 feet off to the side of the test article and 15 feet behind, looking directly into a mirror stand mounted to the concrete test pad. This was the camera positioning for the first several tests. Near the end of the test series the camera looking at the mirror stand was repositioned to view a side profile of the thrust chamber. The third camera had a lower framerate capability than the others and was thus used for the opposite side profile in color to capture any hardware related issues throughout the full duration of the test. It was determined that a sample rate of 150,000 samples per second was optimal, however a lower rate could have allowed for a longer duration video and was only limited by the internal storage capacity of the camera. The average camera duration was between 5-9 seconds for all tests. All cameras were triggered either at “igniter Pc OK” or at “ignition detect” depending on the test. There was also a delay for triggering which was frequently used depending on the individual test goals.

IV. Discussion of Results

Hot fire testing was conducted with two different bipropellants (LOX/GH2 and LOX/CH4). The previously described AM hardware was evaluated with long duration burns up to 133 seconds and numerous throttle points at varying mixture ratios. The LOX/GH2 phase started in June 2022 with the calorimeter V1 chamber. After testing this configuration, the hardware was changed to the axial channel integrated V2 configuration. The Alloy 718 injector was paired with this chamber. 12 hot fires were attempted with the V1 and one test, 013, with the V2 chamber. During test 013, the inner body experienced a burn-through of the hot wall due to powder clogging of the coolant channels. No CT scanning was performed before manufacturing due to time constraints and posttest analysis found substantial powder entrapment throughout multiple channels in the part. This completed the hydrogen test phase. All tests with LOX/GH2 used the previously described externally mounted CASI for ignition, where the igniter combustion products were redirected through tubing pointing directly into the annulus. Hot fire statistics of these hardware are given in Table 3 and Table 4.

Table 3. Hot fire statistics of hardware– Phase 1 hydrogen testing.

Hardware Description	Material	Total Duration (s)	Starts
MER05651 Injector Assembly	GRCop-42	357	8

MER05415 V1 Chamber Assembly (calorimeter)	GRCop-84	357	8
MER05419 Aerospike 30 Cone	GRCop-42	357	8
MER05651 Injector Assembly	Alloy 718	0.5	1
MER05423 V2 Inner Body	GRCop-84	0.5	1
MER05426 V2 Outer Body	GRCop-84	0.5	1

Phase 1 testing resulted in 357 seconds of total duration at 8 hot fire starts. No wave modes were imaged via high-speed during the 012 hot fire attempts.

Immediately following buildup for phase 2, testing began towards hot fire evaluation of hardware with regenerative and direct injection LOX/CH4 and LOX/LCH4, respectively. The LOX/CH4 phase started in July 2022 with the V2 chamber. As previously shown in Table 2, methane was gasified by absorption of heat load from the V2 outer body or the V1 inner body and plug nozzle. The final three tests, 026-028 utilized direct injection of liquid methane and liquid oxygen in the V1 hardware. Engineers evaluated the hardware with long duration burns up to 133 seconds for a single burn with liquid/liquid injection. After testing this configuration, the hardware was changed to the V1 hardware. All tests with methane V2 hardware were ignited using the integrated multi-point CASI where oxygen rich combustion products were transported into the annulus via igniter ports within the face. When the configuration was switched to the V1, external CASI ignition was again utilized. Hot fire statistics of support hardware under Phase 2 methane testing are shown in Table 4.

Table 4. Hot fire statistics of support hardware under Phase 2 methane testing.

Hardware Description	Material	Total Duration (s)	Starts
MER05859-005 Injector Assembly	GRCop-42	112	1
MER05859-003 Injector Assembly	GRCop-42	85	2
MER05423 V2 Inner Body	GRCop-42	197	3
MER05426 V2 Outer Body	GRCop-84	197	3
MER05415 V1 Chamber Assembly (calorimeter)	GRCop-84	248	7
MER05419 Aerospike 30 Cone	GRCop-42	248	7

Phase 2 testing resulted in 445 seconds of total duration at 10 hot fire starts. Of which, 193 seconds were achieved with 3 starts in direct liquid/liquid injection with waves imaged throughout each test. The majority of tests were found to have wave direction in the clockwise or counterclockwise direction, which was detected via high-speed imaging at select times throughout each test. Ultimately, the test series achieved a total of 802 seconds of total duration at 18 starts. It is estimated that the V1 and V2 chambers were subjected to approximately 1.5-2.5 million cycles each.

D. Notable Hot Fire Test Observations

Phase 1 testing began with propellant blowdowns, leak checkouts, purges, and ignition tests to validate all experimental measurements prior to the first hot fire attempt. The first few tests were short duration “burp” tests up to approximately 3 seconds in duration. Once thermal steady state conditions were identified to be below burnout heat loads, then supply pressures and durations were increased. Images of typical ignition and thermal steady state conditions are shown in Fig 11.

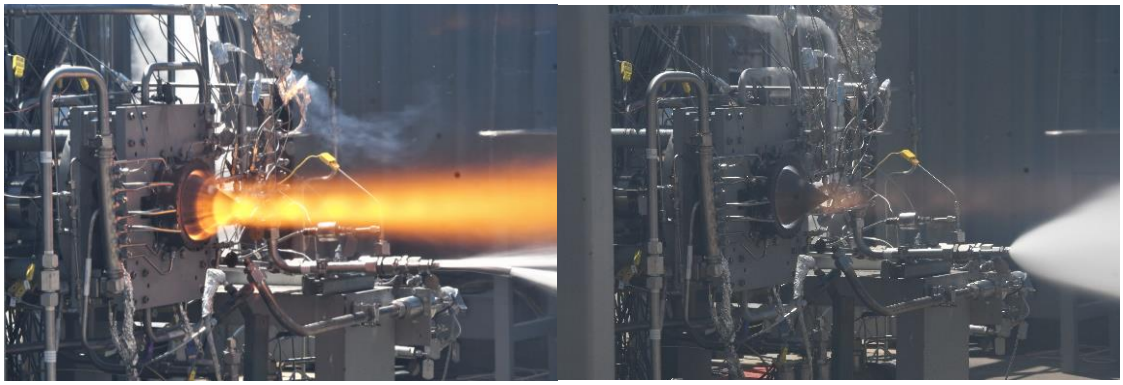

Fig 11. V1 calorimeter hardware first successful ignition (left) and long duration mainstage (right).

The longest mainstage duration the V1 hardware experienced was 113 seconds with LOX/GH2. Streaking from the injector's LOX impingement on the inner and outer walls was observed but not unexpected. In addition, it was not visually more severe than what the authors have observed in CP combustion chambers previously. No blanching was observed on any hardware either. There was some burning, and pitting found at the tip of the plug nozzle after test 007 but did not worsen after it was discovered. Images of streaking and the nozzle tip are shown in Fig 12.

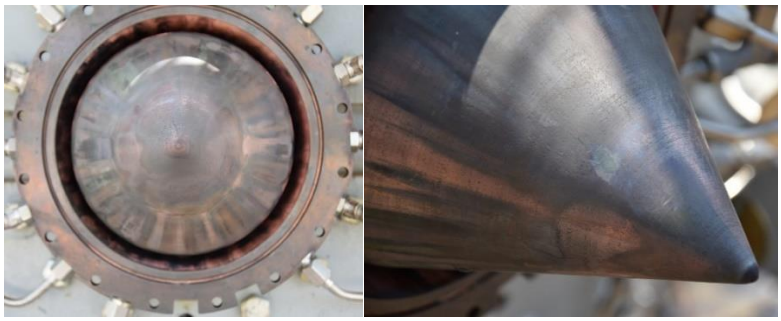

Fig 12. V1 hardware streaking (left) and tip burning and erosion (right).

A single test day was allocated for hot fire evaluation of the V2 hardware with hydrogen. When the test was initiated, a series of events occurred that led to the burn through of the V2 inner body approximately 1.25 inches from the injector face. Ultimately it was determined that the inner body was clogged with powder via computer tomography (CT) scanning which was the primary cause of the burn through and did not become clogged when subjected to hot fire conditions. However, the severity of clogging was far greater than previously expected and not just localized near where the burn through occurred.

CT scans indicate that multiple channels were compromised and likely could have led to further burn throughs if the test had continued. However, the Alloy 718 injector was also found to be substantially eroded on the face, likely due to recirculation zones of combustion products. This is not something observed previously with constant pressure engines and may indicate that the heat loads the injector face is subjected to is no longer just the radiative component of heat transfer. This caused the plume to glow bright yellow and deposit molten metal along the relatively cooler wall downstream. Solidified deposits were found on the outer body, which was unharmed and reused in phase 2 testing, in addition to the location where the burn through occurred on the inner body. This deposition may have caused the initiation of the burn through. This may also have implications for material compatibility for future hardware development, where specific injection schemes or engine cycles may be preferred with specific metals depending on the application. Images of the hardware burn through during and after hot fire are shown in Fig 13.

Fig 13. Hot fire burn-through of the V2 inner body.

Similar to Phase 1 testing, Phase 2 testing conducted leak checks, propellant blowdowns, purges, and water blowdowns prior to the first methane hot fire. For the first 3 test attempts, several redlines were tripped while ideal ignition conditions were explored. The first successful ignition resulted in 4-5 co-rotating waves during mainstage level 2. In addition, it was found that the ignition phase prior to the introduction of methane fuel showed wave activity with co and counter rotating modes. At this point in the sequencing, only the preinjected hydrogen and oxygen were within the annulus. Images of this are shown in Fig 14.

Fig 14. LOX/GH2 3 corotating wave modes at mean chamber pressure of ~15 psig and MR = ~15.

After this event, each predefined throttle point achieved steady state conditions.

Immediately following this test, a full power condition was attempted. This test achieved full power based on the facility limitations. The maximum chamber pressure reached 622 psia with a measured thrust of around 4171 lbf. To the authors' knowledge, this is the highest operating pressure with confirmed wave modes in an RDRE based on the available literature. Visual confirmation of wave activity is shown in Fig 16. Sometime during full power mainstage, water was observed leaking into the plume from the inner body. An image of the full power mainstage is shown in Fig 15.

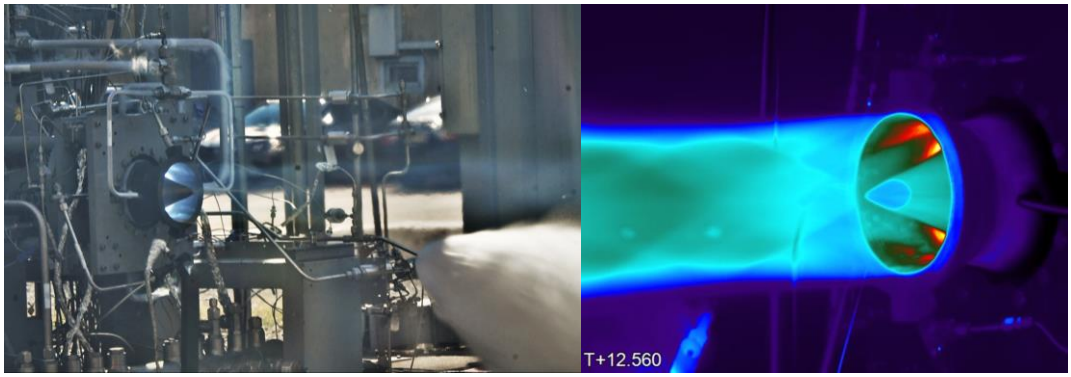

Fig 15. Full power image of test 019 hot fire using the V2 chamber (left) and IR image of plume structure (right).

This case showed between 3-5 waves while the high-speed camera was active. However, there was substantial deflagration and luminosity between the wave heads when viewed from the front end of the thrust chamber.

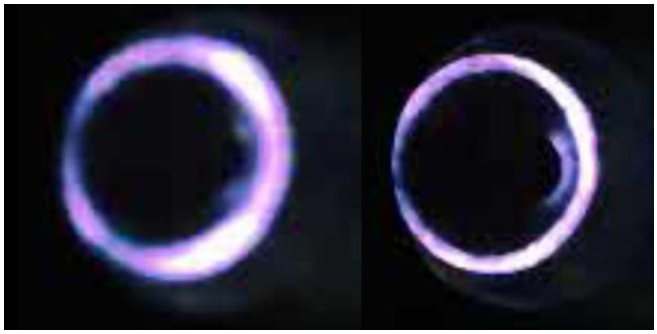

Fig 16. 4 and 3 co-rotating waves at mean chamber pressure of 622 psia in the V2 chamber.

After this test, the V1 hardware was reintegrated into the test stand and subsequent configurations presented in Table 2 were explored. Wave modes were observed for several tests thereafter with a handful of others showing only deflagration in the flow field. In addition, the complexity of the hardware caused substantial leakage of cryogenic methane and initiated fires approximately 10 seconds into each test, after which the test was manually cut. An example of which is shown Fig 17.

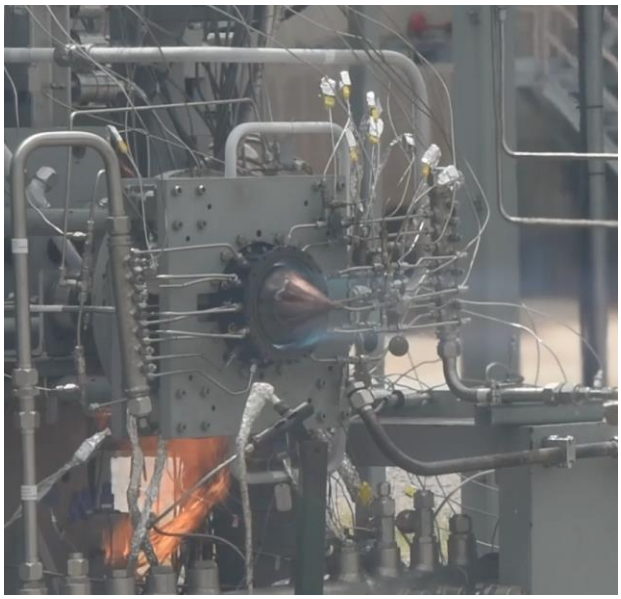

Fig 17. Test 021 fire at bottom left of the test article.

On the last day of testing, the final configuration change was made for direct injection of liquid oxygen and liquid methane. In total, three liquid/liquid tests were achieved with all containing detonation activity at various throttle points and mixture ratios. Liquid methane and oxygen were confirmed through density calculation in the respective manifolds. Waves were observed in the high-speed data and are shown Fig 18 from a side profile vantage and looking directly into the annulus.

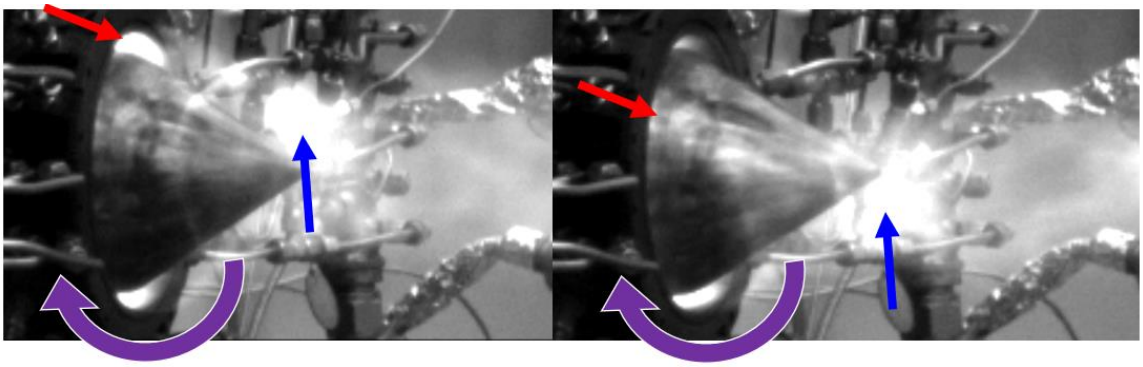

Fig 18. Side profile high speed images (frame by frame) of nozzle wave activity propagating clockwise around the annulus with red arrow indicating leading edge of the wave, blue arrow indicating resultant shock at the nozzle tip, and purple arrow indication direction of rotation.

Fig 19. High speed images of liquid/liquid LOX/LCH4 co-rotating waves. Images show from left to right a frame-by-frame capture of the wave movement.

Throughout this test, 2-3 co-rotating waves were observed. There were some instances where counter propagation would occur but then transition to rotation in the opposite direction. This switching of direction would occur several times within a single hot fire. After the first test, a small amount of water was observed leaking through the chamber during leak checkouts. Test 027 pre-checkouts found that the chamber leak was more noticeable and was severe at ignition and shutdown of test 028. Unfortunately, all chamber pressure ports were frozen throughout the duration of each liquid/liquid test and thus mean chamber pressure was not obtained. Images of the water leakage before each test and during the full power level are shown Fig 20.

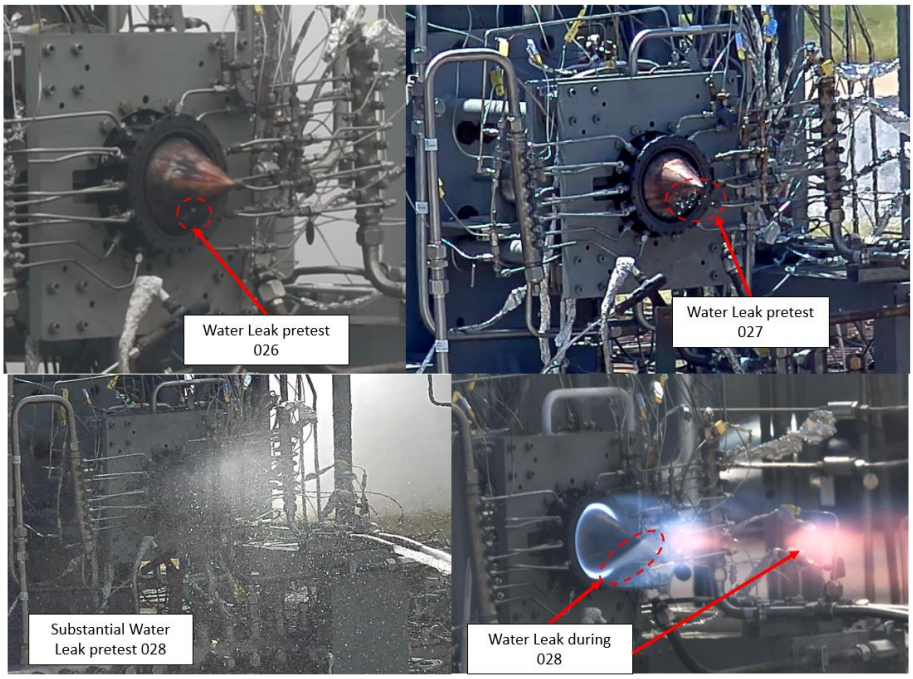

Fig 20. Images of pretest 026-028 and during test 028 of water leakage through the test article.

Regardless of leak severity, the thrust chamber was able to ignite and proceed to each throttle point. During test 028, the leak was so bad that a noticeable change in plume coloration was observed going from a light blue to a red/orange hue. This is likely caused by the high water content in the plume but may also be impacted by unburnt fuel. This test achieved a total duration of 133 seconds and resulted in the completion of the test series. An image of this high-power test is shown in Fig 21.

Fig 21. High power liquid/liquid direct injection at MR 3.47 and estimated mean pressure of 330 psia.

V. Phase 1 – Hydrogen Experimental Results

The hydrogen test phase was intended to be a preliminary series of hot fires to evaluate all hardware under constant pressure combustion environments while simultaneously overcooling hardware with deionized (DI) water. No wave activity was expected or observed throughout this phase and was seen as an opportunity to obtain constant pressure data for direct comparison with detonative cases expected in the methane test phase. With that said, it was anticipated that detonation cases would cause heat fluxes much higher than constant pressure cases. Thus, starting with overcooling using DI water would give the authors a baseline for calculating coolant exit temperatures with regenerative methane.

NASA test stand 115 at MSFC has the capability of directly injecting gaseous hydrogen fuel up to about 1 lbm/s at a maximum source pressure of 2700 psi. This was not possible with methane since it is delivered in liquid cryogenic form and was the primary fuel of interest for the test campaign. To gasify, the only feasible method is routing through a regen circuit. Direct injection of liquid methane and liquid oxygen was expected to cause extreme heat fluxes from pressure waves beyond what the hardware could handle. This was found not to be the case with GRCop-alloys.

The hot fire map of tests conducted is shown in Fig 22. Mean chamber pressure was measured at the injector face via sense-line. This way the total pressure could be captured and directly compared to constant pressure thrust chambers previously tested by the Engine Components Development and Technology Branch at NASA MSFC. As shown in Fig 22, a wide range of mixture ratios and mean chamber pressures were explored. Two regimes are shown delineated by mixture ratio where the higher MR cases were intended to explore more ideal injection conditions to produce wave modes.

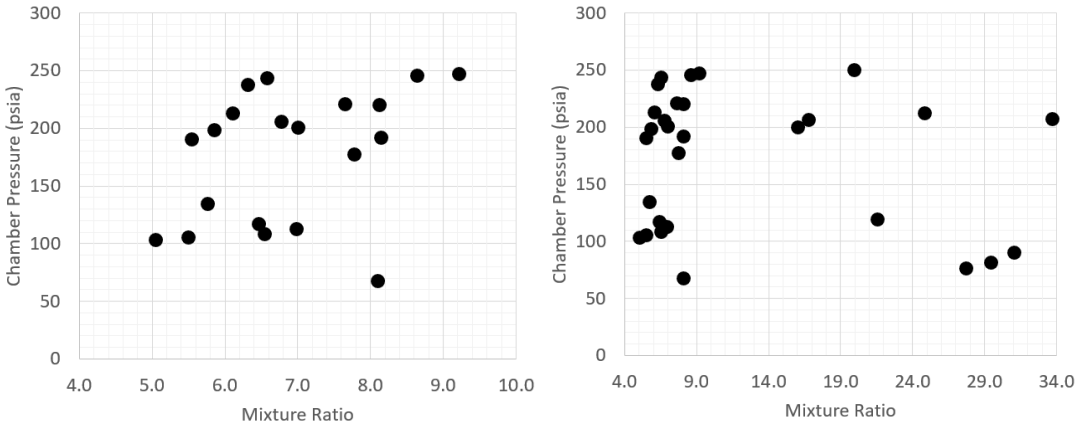

Fig 22. Map of tests conducted under Phase 1 hydrogen testing, low MR range (left) and high range (right).

A. Infrared Imaging of Plume Dynamics – Hydrogen

For the majority of the phase 1 tests the V1 plume appeared to be under expanded forming two or more shock halos along the nozzle below about 130 psia mean chamber pressure. At about 150 – 170 psia, the shock anchors at the tip of the nozzle and remains there until a mean chamber pressure of about 220 psia where it blends to an even green where the flow appears as if it were near-ideally expanded as the nozzle geometry would allow. Beyond this point, the flow is over expanded forming a normal shock just downstream of the nozzle tip. Pressures closer to 260 psia push this shock out past the plug nozzle tip. The reader should note that vertical lines in all IR images are physical structures in the background.

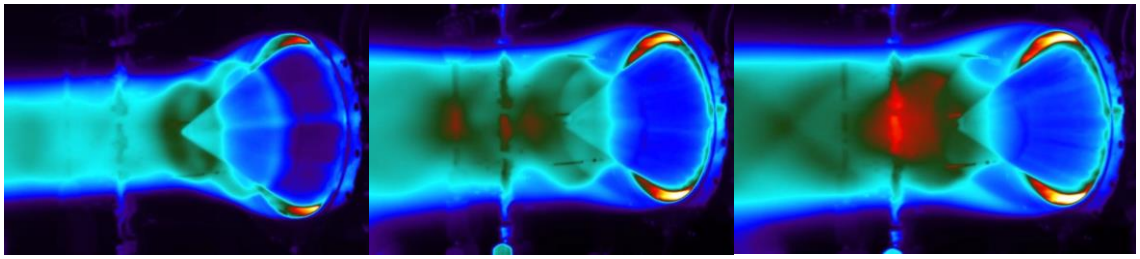

Figure 23. IR imaging of Phase 1 test 007 at various throttle points of 108, 205, and 247 psia mean chamber pressure.

A major observation for this design during testing is the "bulge" of rapidly expanding gases right at the exit plane of the cowl. For lower pressure cases, this is not significant feature, however it is clearly shown in higher pressure cases. This is similarly the case with methane tests presented in Fig 24.

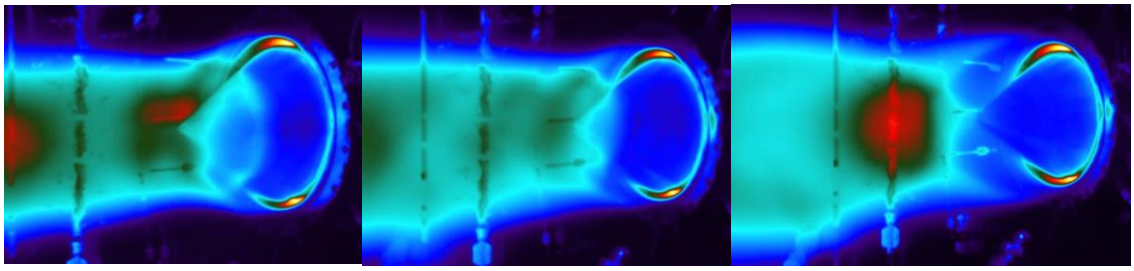

Fig 24. IR imaging of Phase 2 methane test 028 at assumed throttle points of 127, 186, 330 psia mean chamber pressure.

The throat cross sectional area is 6.137 in^2 while the exit plane at the cowl is 8.607 in^2 allowing for a slight expansion of the flow along the plug and cowl before contacting atmosphere. It is expected that since no cowl is intentionally redirecting the flow down the plug nozzle, there may be regions of appreciably low pressure along the nozzle. This is particularly a concern for high thrust cases and would theoretically reduce the measured Isp of the thrust chamber. This has also been reported to be the case in studies such as [9] with a similar nozzle geometry. These observations underline the need for a direct study on the design for detonation cycle engine nozzles.

VI. Phase 2 – Methane Experimental Results

Once the hydrogen test phase was completed, the hardware was changed out to the V2 chamber configuration. The performance map of conditions tested for both gas and liquid methane are shown in Fig 25.

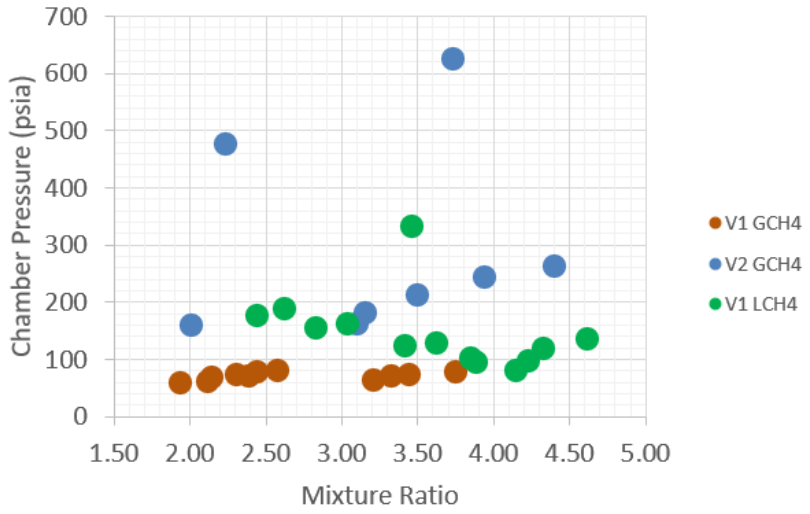

Fig 25. Map of test conditions for methane phase 2 testing.

A. Infrared Imaging of Plume Dynamics - Methane

Test 019 was an excellent case study particularly at ignition to mainstage level 2 where wave activity was observed in the high-speed imaging. Both high speed and IR stills are shown in Fig 26 of this ignition phase.

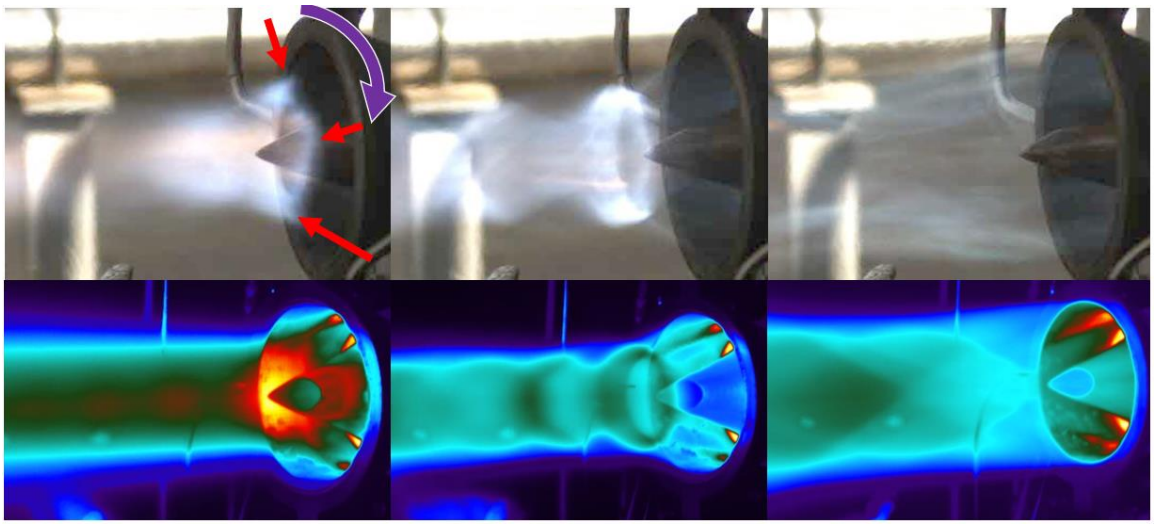

Fig 26. High speed and IR still images at ignition to full power mainstage.

The major observation from these imagery and videography is that while the flow was separated from the outer nozzle the wave rotation attached to the inner body plug nozzle could clearly be seen in the high speed. A single still of this is shown in the top left of Fig 26 with the four oblique shock heads from the 4-wave case. Once the flow attaches to the outer body nozzle, the oblique shock rotation in the plume is substantially diminished and the plume appears to resemble a typical liquid rocket plume. Shock structure can be seen downstream of the plug nozzle. Past this point, the plume pushes to near ideal expansion as full chamber pressure is achieved. To further explore the topic of plume structure, the following figure directly compares imagery of a test case with wave structure versus a deflagration dominated plume at a similar mean chamber pressure.

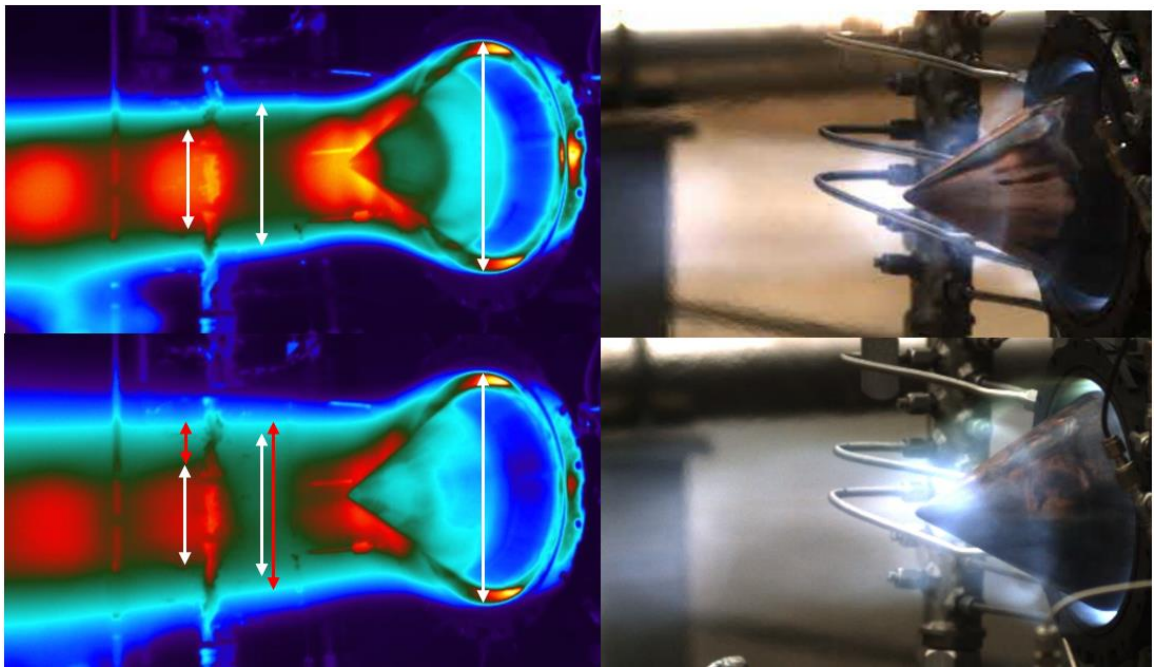

Fig 27. Test 024 level 6 LOX/GCH4 at 76 psia (top) and test 027 level 2 LOX/LCH4 at 92 psia (bottom).

Fig 27 directly compares a constant pressure test with a deflagrative test, 024 – MR: 3.75 and 027 – MR: 3.9, respectively. They are of similar mixture ratios and chamber pressures. Right away it is clear that the shock structure from the under expanded flow are roughly in the same location indicating that mean chamber pressure is roughly equivalent. The arrows provided on the IR frames indicate direct measure of scale. All white arrows are of identical length while red arrows point out major differences in scale. For example, the downstream shocks are of the same width, but the green shear layer is thicker for the case with waves. Furthermore, the overall thickness of the plume is larger at the same cross section for the detonation case. The first shock at the plug nozzle tip appears to be behind the nozzle for the detonation case while it appears to encompass the nozzle for the deflagration case. This is found to apply to all frames in the IR videography.

The last observation that can be made is the luminous intensity of the combustion products at the nozzle exit as shown in Fig 27. The plume is clearly brighter for the case with waves; however, it is unclear how this relates to performance. It is the experience of the authors that plumes at higher chamber pressures for constant pressure engines are greater in luminous intensity. An example of this is shown in Fig 28 for the NASA LLAMA engine in LOX/CH4 propellants at varying throttle points.

Fig 28. LLAMA lander engine throttle test from mean chamber pressures of 130 psia (left) to 350 psia (right) with LOX/CH4.

This could be an indication of higher combustion performance in the chamber with higher temperature exhaust or it could be an indication of lower completion of combustion due to unburned fuel in the exhaust.

B. Wave Activity and Performance

The primary objective of this work was to demonstrate long duration firings at high thrust with additive L-PBF GRCop-alloy components and demonstrate survivability. This objective was met along with several other secondary objectives. Confirmation of wave activity was achieved both passively and actively through various instrumentation. First and most importantly, high speed phantom cameras were used to directly capture the wave motion with subsequent parameters such as velocity, frequency, wave mode type, and number of waves captured in post processing. High speed pressure transducers captured the unsteady pressure within both the fuel and oxygen manifolds. All high-speed pressure transducers were connected to 3-foot-long sense-lines. The transducers used to measure the mean chamber pressure were connected to 4 evenly spaced ports printed directly into the injector face. All high-speed data were collected at the maximum facility sample rate of 100K samples per second.

Since many of the tests conducted were 10 to 100 seconds in duration, only a fraction of the test data was visually confirmed to have wave activity. In addition, due to the complexity, number of challenges, and scale of the hardware, wave activity was often only captured at the engine startup and rarely within the thermal steady state. Several different wave modes were observed at startup ranging from 2-4 wave counter propagating modes, one through five wave co-rotating modes, and two wave slapping modes. No longitudinally pulsed modes were observed in any test. Only select cases where wave activity was captured at thermal steady state are presented in Fig 29 and Fig 30.

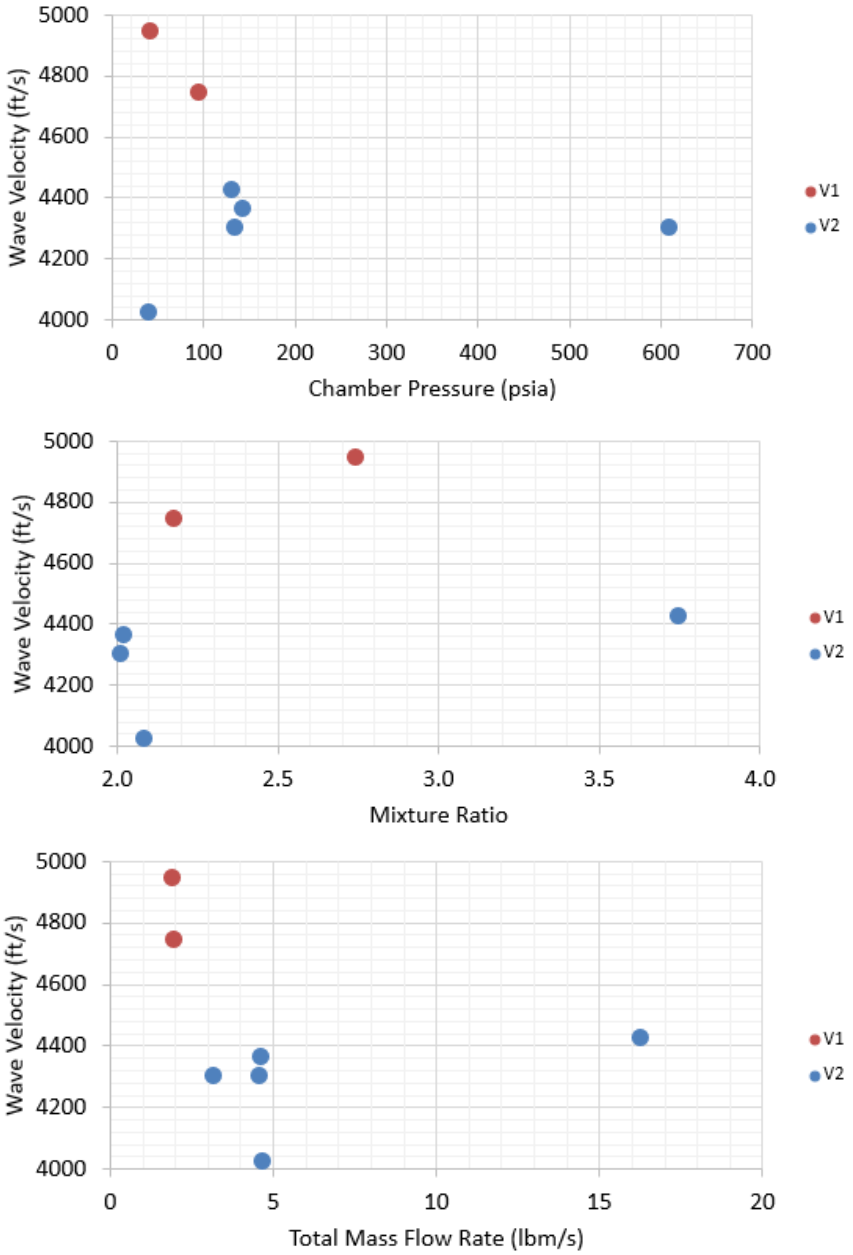

Fig 29. High speed imaging measured wave velocity as a function of mean chamber pressure, mixture ratio, and total mass flow rate of propellant for the V1 and V2 hardware.

All test cases using LOX/GCH4 injection showed wave velocities between 4000 and 5000 feet per second. In general, the V1 configuration showed slightly higher velocity modes but may not be statistically significant given the number of data points presented.

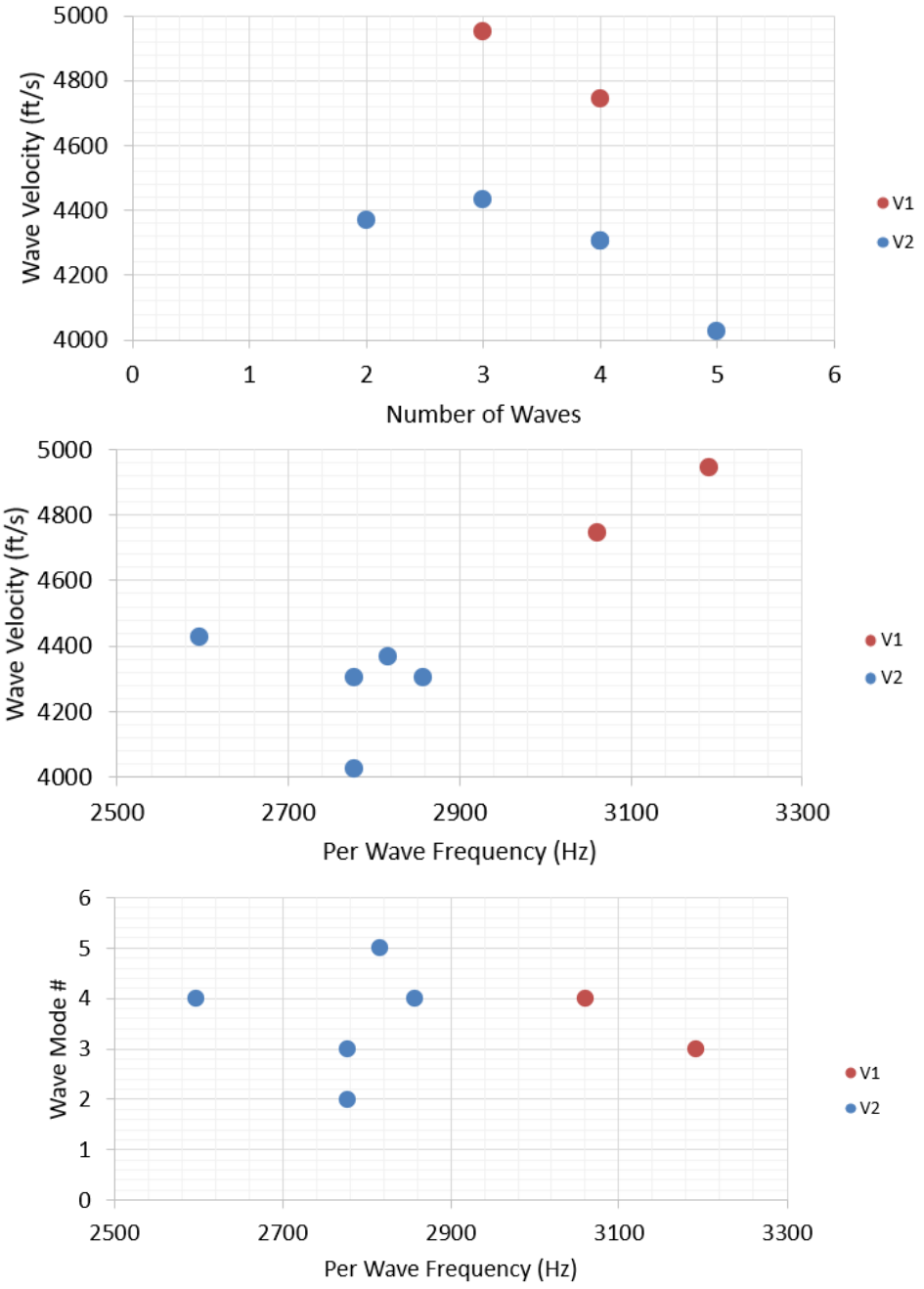

Fig 30. Wave velocity, number of waves, and per wave frequency for the V1 and V2 chambers.

There also appears to be no correlation between thrust chamber performance parameters and wave performance parameters. Thus, control over wave mode operation may not be necessary or useful from a design standpoint.

The liquid/liquid testing was similar in findings but had no coherent trends with wave activity. For example, test 026 captured mainstage level 2 and 3 at an estimated 100 and 117 psia at mixture ratios of 3.86 and 4.34, respectively. During level 2, 4-corotating modes were observed in the clockwise direction that then quickly transitioned to 3 corotating modes in the counterclockwise direction. The 3-wave case velocity was about 5400 feet per second at a

single wave frequency of 3846 Hz. A few seconds later the thrust chamber transitioned to a 2-wave corotating mode at velocity of nearly 6000 feet per second and single wave frequency of 3850 Hz. Once the throttle point changed to level 3, the engine transitioned back to a 3 wave corotating mode at a velocity of 4400 feet per second and single wave frequency of 2800 Hz. There was a continuous transition between clockwise and counterclockwise throughout the duration of the test. Over the 9 seconds of recorded high-speed data, this transition occurred more than a dozen times.

Similarly, test 027 saw nearly the identical process unfold at similar wave velocities and frequencies. Test 028 recorded the transition between mainstage level 5 to the high-power level 6. Level 5 and 6 were estimated to have mean chamber pressures of 186 and 330 psia at a 2.63 and 3.47 mixture ratio, respectively. Again, similar wave activity was observed where a transition from a 3-wave corotating mode to a 2-wave corotating mode occurred. However, the 2-wave mode was substantially lower in velocity at 3520 feet per second down from 4230 feet per second during level 5. Consequently, this was also when a substantial amount of water was observed leaking into the annulus and visible along the nose of the plug nozzle. It may be that the introduction of a diluent caused a decrease in wave velocity. Later in the test, it was observed that more chaotic modal transitions were occurring as more water was introduced into the annulus. 2-wave and 3-wave modes with counter propagation were found to dominate. Example images of the observed waves are shown in Fig 31.

Fig 31. 3-wave (left) and 2-wave (right) corotating modes observed in test 026 and 028, respectively.

One key feature worth noting between each test was that as the total mass flow rate increased, the luminosity of the wave heads also increased.

VII. Summary and Conclusions

Hot fire testing of NASAs first high thrust continuously rotating detonation rocket engine hardware was conducted during the summer of 2022. Two propellants were explored, LOX/H2 and LOX/CH4, where hydrogen was injected in a gaseous state and methane was injected in both gas and liquid states. Two annular chamber geometries were designed with integrated cooling channels and produced using the additive manufacturing laser powder bed fusion process. The primary materials used were GRCop-42 and GRCop-84. Several technology advancements were successfully demonstrated, and major conclusions could be drawn from this effort and are as follows.

1. The primary objective was to demonstrate continuous detonation modes within AM GRCop-alloy regenerative hardware was achieved. In summation, 802 seconds of total duration and 18 total starts were achieved. Several long duration firings were also demonstrated in all three propellant combinations up to 133 seconds for a single burn, both with and without visual confirmation of wave modes.
2. A new configuration of augmented spark ignition was used in conjunction with the NASA compact augmented spark igniter (CASI). This is referred to as multi-point ignition. It has been commonplace in the community to externally ignite (backlighting) or pass a predetonator tube through the hot wall or chamber throat. These ignition methodologies are likely not viable for future flight hardware requiring integrated cooling channels and vacuum operation. Thus, a new robust and high-reliability ignition method was developed. Several tests were successfully ignited internally without the need for an external ignition source.
3. Combustion performance, or rather completion of combustion, was found to be equivalent to a constant pressure operating thrust chamber but with L* and L' an order of magnitude smaller.
4. The V1 hardware successfully demonstrated wave mode activity using LOX/CH4 with methane directly injected as liquid or gas phase. Regardless of mixture ratio or mean chamber pressure, 2-5 waves were present in the combustor. All wave parameters were found to be independent of mean chamber stagnation pressure and mixture ratio.
5. A single hot fire with the V2 configuration using LOX/GCH4 injection achieved a mean chamber pressure of 622 psia and 4171 lbf.

Future Work

Future efforts will need to reduce the risk of key RDRE technology areas. Many of which will be explored under follow on work funded by NASAs Space Technology Mission Directorate (STMD) during FY23-24. These include investigation of:

1. Injection magnitude of stiffness and ratio of stiffness. It is not known if a specific stiffness ratio is required for high performance. In addition, high stiffness injection is not practical for flight engines. Stiffness closer to 100% down to 50% $\Delta P/P_c$ at mean chamber pressures approaching 1000 psia will be targeted, though a lower pressure geometry may prove to be more ideal for a vacuum optimized space engine.
2. Ignition with even distribution of combustion within the annulus is required to reduce deleterious impacts of hard start and extended lengths required for DDT.
3. Self-sustained cooling utilizing only propellants will need to be demonstrated.
4. Nozzle design for annular geometries in addition to the detonation cycle will need to be experimentally and computationally investigated to produce the highest possible performances and minimize losses.

Acknowledgments

This work has given numerous student engineers the opportunity to learn and expand their knowledge base within NASA. These students include Michaela Hemming (NSTGRO Fellow), Nate Ballintyn (NSTGRO Fellow), Cory Marquez (GEM Fellow), Ari Goldman (AL Space Grant Fellow), Dillon Petty (NASA Pathways), and Jaiden Stark (NASA Pathways). Without these students' assistance, the numerous accomplishments described in this work would not have been possible. The author would also like to thank the collaborators including but not limited to IN Space, LLC, Purdue University, Elementum 3D, Quadrus Corp., AME, NASA ET10, NASA STMD, and the profound support amongst the pressure gain community.

References

[1] T. W. Teasley, P. R. Gradl, M. B. Garcia, B. B. Williams, and C. S. Protz, "Extreme Environment Hot Fire Durability of Post Processed Additively Manufactured GRCop-Alloy Combustion Chambers," in *AIAA Propulsion and Energy 2021 Forum*, 2021, p. 3233.

[2] T. W. Teasley, P. R. Gradl, M. B. Garcia, B. B. Williams, and C. S. Protz, "Hot Fire Test Durability of Post Process Polished Additively Manufactured GRCop-Alloy Combustion Chambers in LOX/Methane and LOX/Hydrogen," *Jt. Army Navy NASA Air Force*, no. 0001BN, 2021.

[3] S. E. Greene, "Test Summary Report for PJ030: Modified Methane Engine Thrust Assembly for 4K lbf with a 4" Diameter Chamber (META4X4)," Huntsville, AL, 2020.

[4] T. W. Teasley, "Test Summary Report for Test Program PJ062 "1.2K GRCop Chamber and HR-1 Nozzle Cycle Testing"," Huntsville, AL, 2021.

[5] T. W. Teasley and P. R. Gradl, "PJ116 Test Summary Report - Composite Overwrap Methane Engine Thruster (COMET) GRCop-42 7K lbf LOX/Methane Testing," Huntsville, AL, 2021.

[6] T. Teasley, "Test Summary Report for PK129: Cycle Testing of GRCop-42 Long Life Additively Manufactured Assembly (LLAMA) 7K lbf Phase 2," Huntsville, AL, 2021.

[7] T. Teasley, "Test Summary Report for Test Program PK058 & PK129 "Cycle Testing of 7K lbf GRCop-42 Long Life Additively Manufactured Assembly (LLAMA)"," Huntsville, AL, 2021.

[8] E. C. Unruh, M. Spaulding, D. M. Lineberry, K. G. Xu, and R. A. Frederick, "Development of an Optically Accessible Racetrack-Type Rotating Detonation Rocket Engine," in *AIAA Propulsion and Energy 2020 Forum*, 2020, p. 3868.

[9] K. Miki, D. E. Paxson, D. Perkins, and S. Yungster, "RDE Nozzle Computational Design Methodology Development and Application," in *AIAA Propulsion and Energy 2020 Forum*, 2020, p. 3872.